Science Bulletin 70 (2025) 483–487

Contents lists available at ScienceDirect

Science Bulletin

journal homepage: www.elsevier.com/locate/scib

Short Communication

Impaired tactile processing in autism-associated *Shank3* mutant dogs: neural mechanism and intervention

Qi Shi [a,b], Liang Wu [a], Baolong Ren [a,c], Kun Guo [d], Yong-Hui Jiang [e,f,g], Yong Q. Zhang [a,b,h,*], Li Hu [i,j,*]

[a] State Key Laboratory for Molecular and Developmental Biology, Institute of Genetics and Developmental Biology, Chinese Academy of Sciences, Beijing 100101, China
[b] College of Life Sciences, University of Chinese Academy of Sciences, Beijing 100049, China
[c] Sino-Danish College, University of Chinese Academy of Sciences, Beijing 100049, China
[d] School of Psychology, University of Lincoln, Brayford Pool, Lincoln LN6 7TS, UK
[e] Department of Genetics, Yale University School of Medicine, New Haven, CT 06510, USA
[f] Department of Neuroscience, Yale University School of Medicine, New Haven, CT 06510, USA
[g] Department of Pediatrics, Yale University School of Medicine, New Haven, CT 06510, USA
[h] School of Life Sciences, Hubei University, Wuhan 430415, China
[i] CAS Key Laboratory of Mental Health, Institute of Psychology, Chinese Academy of Sciences, Beijing 100101, China
[j] Department of Psychology, University of Chinese Academy of Sciences, Beijing 100049, China

ARTICLE INFO

Article history:
Received 3 May 2024
Received in revised form 2 July 2024
Accepted 5 September 2024
Available online 10 September 2024

Sensory processing anomaly is a common co-morbidity associated with Autism Spectrum Disorder (ASD). While the prevalence of altered sensory responses is reported in up to 90% of ASD individuals [1], sensory processing abnormalities exhibit considerable heterogeneity of either heightened or reduced reactivity to various stimuli, including tactile [2]. Despite the significance of sensory issues, the cause and pathophysiology underlying sensory abnormalities in ASD individuals remain largely unknown. Mutations in *SHANK3* are one of the most common genetic causes of ASD. Besides highly penetrant autism core behaviors, sensory processing issues are reported commonly in individuals with *SHANK3* genetic mutations. Approximately 75% of individuals with *SHANK3*-associated disorders have sensory processing issues, including under-responsiveness to tactile stimuli, increased pain tolerance, and other sensory issues related to smell, taste, vision, and audition [3]. Opposite to the reduced tactile response in patients carrying *SHANK3* mutations [3], increased [4,5] or unaltered [6] responses to tactile stimuli in *Shank3* isoform-specific mutant mice were observed. The exact reasons behind the inconsistent tactile phenotypes in *Shank3* mutant mice and patients carrying *SHANK3* mutations remain unclear; these could be attributed to differences in species, individual experiences, genotypes, or experimental paradigms (i.e., specific stimuli and target sites).

Although the potential connection between altered sensory processing and core autism behaviors has been investigated in ASD patients [7], the complex presentations of sensory issues and autistic behaviors in human ASD pose a significant challenge to dissect these behaviors in animal models [5,8]. Crucially, whole genome analyses reveal significant convergence in obsessive–compulsive disorders, a comorbidity of ASD, between humans and dogs [9]. We recently generated and characterized a *Shank3* mutant dog model that exhibited impaired social interactions with both conspecifics and humans [10]. With this model, we can delve into the tactile processing abnormalities in *Shank3* mutant dogs. Notably, the somatosensory system including components of the peripheral and central nervous systems sub-serving tactile sensations in domestic dogs closely resembles that of humans [11]. Additionally, the experimental paradigms of tactile detection in dogs are comparable to that in humans, as limb skin is the main site for stimulation in humans and dogs [12]. In the current study, we aimed to investigate sensory processing abnormalities and their underlying neural mechanisms in *Shank3* mutant dogs (Table S1 online). All surgical and experimental procedures, as well as animal care and handling, were approved by the ethics committee at the Institute of Genetics and Developmental Biology, Chinese Academy of Sciences (AP2022033 and AP2024026).

To explore the potential role of *Shank3* in regulating the somatosensory function, we evaluated tactile sensitivity in *Shank3* mutant dogs. By comparing tactile responses to electrical pulses, we observed that the tactile threshold at which a stimulus-

* Corresponding authors.
E-mail addresses: yqzhang@genetics.ac.cn (Y.Q. Zhang), huli@psych.ac.cn (L. Hu).

https://doi.org/10.1016/j.scib.2024.09.011
2095-9273/

induced paw-lifting response in *Shank3* mutant dogs was significantly higher than that in wild-type (WT) dogs (Fig. 1a), indicating reduced tactile sensitivity in *Shank3* mutant dogs. Consistently, *Shank3* mutant dogs exhibited impaired tactile discrimination of different textures (Fig. S1 online).

To assess neural processing to tactile stimuli, we recorded somatosensory evoked potentials (SEPs) using 32-channel electrocorticographic (ECoG) electrodes placed on the right brain hemisphere, covering a full range of cortical regions (Fig. 1b). The largest grand-averaged SEP waveforms, in response to tactile stimuli ranging from 0 to 4 mA in 0.5 mA increments at inter-stimulus interval (ISI) of 800 ms delivered to the left forepaw (Fig. 1c), are observed at the somatosensory cortex for both *Shank3* mutant and WT dogs (Fig. 1d and Fig. S2a online). Grand-averaged SEP

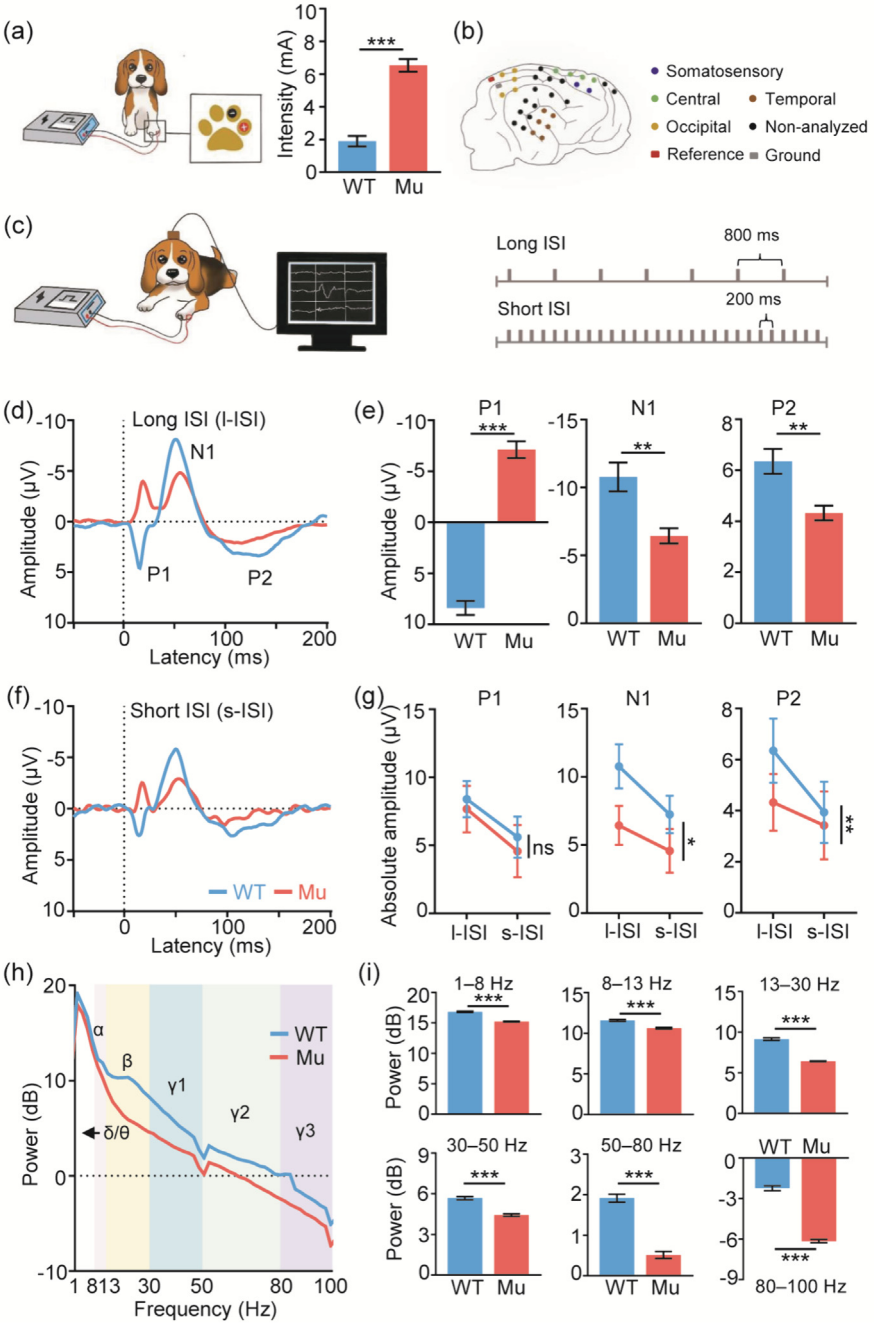

Fig. 1. *Shank3* mutant dogs showed reduced reactivity and neural responses to tactile stimuli. (a) Schematic for tactile sensitivity test with electrical stimuli delivered to the left forepaw at digits 3 and 4. Comparison of tactile threshold between *Shank3* mutant (Mu, n = 13, 6.54 ± 1.39 mA) and wide-type (WT, n = 15, 1.90 ± 1.21 mA) dogs. (b) Schematic displaying the placement of 32-recording ECoG electrodes with the ground and reference covering the right cerebral cortex, contralateral to the stimulated forepaw. (c) Schematic for the recording of cortical responses to tactile stimuli at long (800 ms) and short (200 ms) ISIs in Mu and WT dogs (in each group, N = 6 and 5 for long and short ISIs, respectively). (d) Grand-averaged cortical responses evoked by electrical stimuli at long ISI (l-ISI) in Mu (red) and WT (blue) dogs at the somatosensory cortex (n = 270 blocks for each group). (e) Comparisons of P1, N1, and P2 amplitudes. (f) Grand-averaged cortical responses evoked by electrical stimuli at short ISI (s-ISI) in Mu and WT dogs (n = 225 blocks for each group). (g) Comparisons of P1 (absolute values), N1, and P2 amplitudes for long and short ISIs in WT and Mu groups. Both groups showed adaptation of SEP responses. (h) Group-level spectral powers of resting-state brain oscillations (−450 to −100 ms pre-stimulus) from Mu and WT dogs. (i) Comparisons of spectral powers at different frequency bands (n = 270 blocks for both groups). Mann-Whitney U test, ns: no significance, $^{*}P < 0.05$, $^{**}P < 0.01$, $^{***}P < 0.001$.

waveforms at different intensities were presented (Fig. S3 and Tables S2, S3 online). The short latency of SEPs (e.g., <20 ms of initial response) in dogs supports that cortical, as well as behavioral, responses to electrical stimuli of mild intensities largely reflect tactile (fast conduction), rather than nociceptive (slow conduction), processing. In WT dogs, three major deflections were observed in

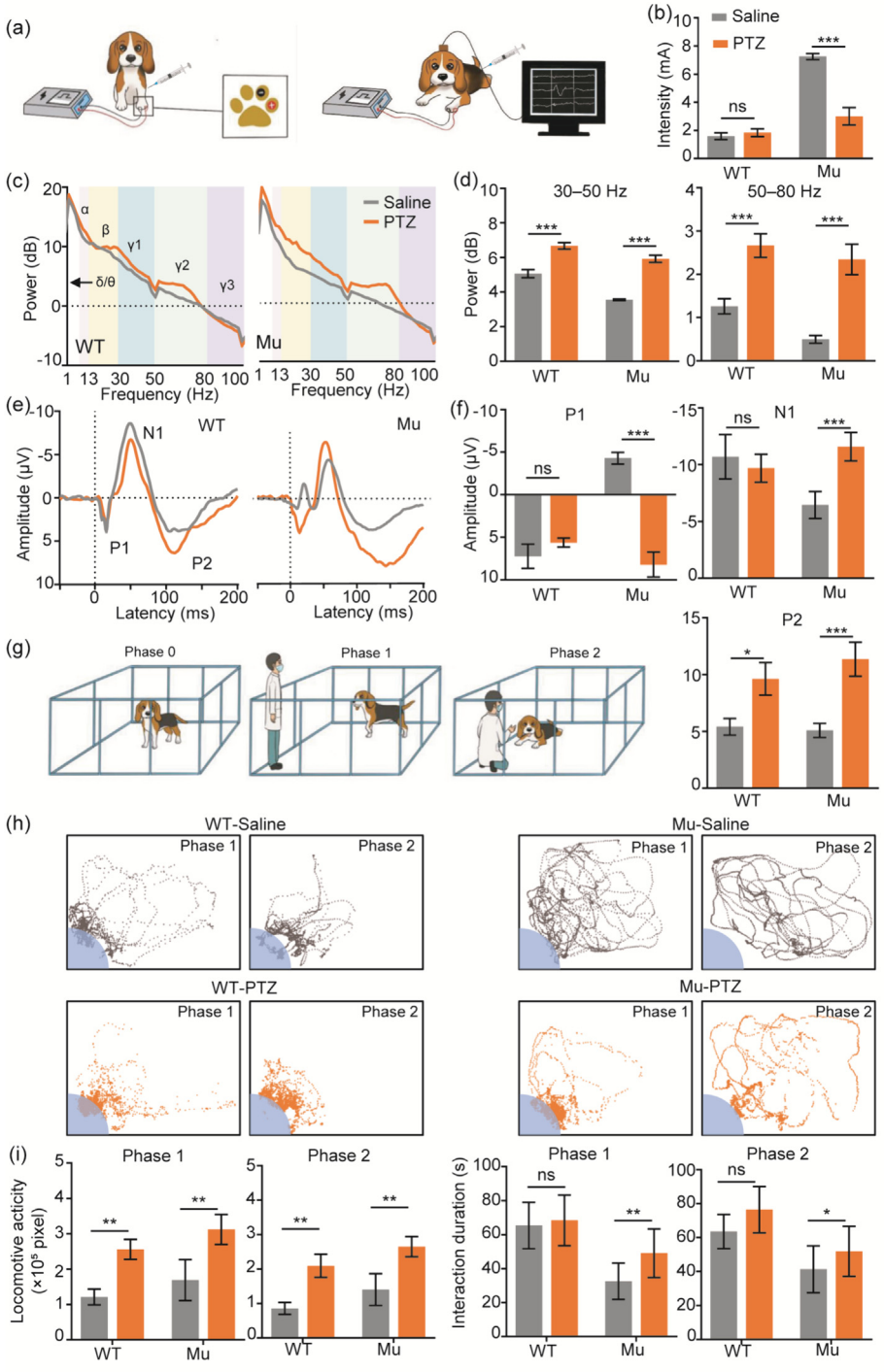

Fig. 2. PTZ ameliorated resting-state brain oscillations, tactile reactivity, and social interactions in *Shank3* mutant dogs. (a) Schematic for tactile sensitivity test (left, n = 6 for each group) and for recording tactile-evoked cortical responses (right, n = 3 for each group) in Mu and WT dogs after saline or PTZ administration. (b) Comparisons of tactile sensitivity between Mu and WT dogs after saline and PTZ administration. (c) Group-level spectral powers of resting-state brain oscillations from WT (left) and Mu (right) dogs after saline and PTZ administration. (d) Comparisons of spectral powers at 30–50 Hz and 50–80 Hz for Mu and WT dogs after saline and PTZ administration (n = 54 blocks each). (e) Grand-averaged cortical responses evoked by tactile stimuli at the somatosensory cortex for WT (left) and Mu (right) dogs after saline and PTZ administration. (f) Comparisons of P1, N1, and P2 amplitudes between Mu and WT dogs after saline and PTZ administration (n = 54 blocks each). (g) Schematic displaying the dog–human social interactions at different phases (phase 0: habituation without the experimenter inside the puppy pen; phase 1: with the experimenter standing in the puppy pen; phase 2: with the experimenter crouching) in Mu and WT dogs after saline or PTZ administration (n = 9 for each group). (h) Representative traces of dog–human social interactions after saline (top) and PTZ (bottom) administration for WT (left) and Mu (right) dogs. The blue area denotes the position of the experimenter. (i) Locomotive activities (movement distance) (left) and interaction duration (right) in the open field test for Mu (n = 9) and WT (n = 9) dogs after saline and PTZ administration. Data are represented as mean ± SEM, two-way ANOVA, ns: no significance, $^{*}P < 0.05$, $^{**}P < 0.01$, $^{**}P < 0.001$.

the somatosensory cortex within 200 ms following electrical stimuli, i.e., an initial sharp positive peak (P1), followed by a negative peak (N1), and a slow positive peak (P2). In *Shank3* mutant dogs, the first P1 peak (observed in WT dogs) was replaced by a later and smaller negative peak (Fig. 1d). Additionally, *Shank3* mutant dogs showed reduced amplitudes and prolonged latencies for almost all waves (Fig. 1e and Fig S2c online), indicating impaired somatosensory processing in *Shank3* mutant dogs.

To verify the abnormal somatosensory processing to tactile stimuli at 800-ms ISI in *Shank3* mutant dogs, we performed a parallel experiment with stimuli at a shorter ISI of 200 ms (Fig. 1f), a time window that contained the majority of SEPs. We also observed a significant reduction in SEP amplitudes in *Shank3* mutant dogs elicited by tactile stimuli when compared with WT dogs (Fig S2b, 2d online). Additionally, the combination of these two experiments allowed us to assess somatosensory adaptation, which was referred to as a reduced response elicited by repeated stimuli with a shorter ISI compared with a longer ISI [13]. *Shank3* mutant and WT dogs showed different adaptation effects, i.e., SEP response differences between short and long ISIs (Table S4 online). Specifically, *Shank3* mutant dogs exhibited significantly smaller decreases in N1 and P2 amplitudes compared with that in WT dogs (Fig. 1g and Table S5 online). These results suggested a reduced adaptation of SEP responses, specifically for N1 and P2 waves, in *Shank3* mutant dogs compared with WT dogs.

Previous studies demonstrated that cortical responses evoked by sensory stimuli could be affected by resting-state brain oscillations occurring before the delivery of the stimuli [14]. To explore the potential that *Shank3* mutant dogs might display abnormalities in resting-state brain oscillations, we compared pre-stimulus ECoG signals in *Shank3* mutant and WT dogs. Spectral powers estimated from pre-stimulus ECoG signals (−450 to −100 ms) using fast Fourier transformation revealed distinctive patterns between *Shank3* mutant and WT dogs (Fig. 1h). Specifically, the spectral powers of pre-stimulus brain oscillations in *Shank3* mutant dogs were significantly lower than in WT dogs at all frequency bands (Fig. 1i), especially for high-frequency gamma oscillations (>30 Hz), although the brain topographies between WT and *Shank3* mutants appeared similar (Fig. S5a online). It is well-established that GABA antagonists can enhance resting-state gamma oscillations [15]. We therefore investigated whether a $GABA_A$ receptor antagonist, such as PTZ, could rescue the reduced resting-state brain oscillations in *Shank3* mutant dogs (Fig. 2a). To determine the optimal PTZ dose, we tested the dose-dependent relationship between PTZ and tactile sensitivity (Fig S4 online). In the formal rescue experiment, we administrated PTZ intramuscularly at 1.5 mg/kg, 10 times lower than the seizure-inducing concentration [16]. Neither *Shank3* mutant nor WT dogs exhibited any signs of seizures during and after the experiment. PTZ significantly increased the spectral powers of resting-state brain oscillations in both *Shank3* mutant and WT dogs, with a stronger modulation for high-frequency gamma oscillations in *Shank3* mutant dogs (Fig. 2c, d, Fig. S5b, and Table S6 online). Notably, PTZ induced more significant increases in the spectral powers of resting-state brain oscillations in *Shank3* mutant dogs compared to WT dogs (Fig. 2c and Table S6 online). PTZ administration also significantly improved the tactile threshold in *Shank3* mutant dogs (Fig. 2b). Moreover, SEPs in *Shank3* mutant dogs were enhanced after PTZ administration, to levels close to the responses observed in WT controls (Fig. 2e, f, and Table S7 online). In particular, the initial negative peak of SEPs in *Shank3* mutant dogs exhibited a reversal in polarity, transforming into a positive wave (P1), similar to the polarity observed in WT controls (Fig. 2e, f, and Table S7 online). These results revealed that PTZ effectively improved both resting-state brain oscillations and tactile reactivity in *Shank3* mutant dogs.

We also investigated whether the PTZ treatment could have any impact on the impaired human–dog social interactions in *Shank3* mutant dogs using a two-phase open-field assay (Fig. 2g). After saline administration, *Shank3* mutant dogs displayed a proclivity for wandering in the two-phase test, devoid of any discernible location preference in the presence of an experimenter as depicted by the traces, while WT controls notably favored proximity to the experimenter; after PTZ administration, both *Shank3* mutant and WT dogs became more locomotive in the presence of the experimenter, with a more pronounced increase in social interaction, e.g., more receptive to social touch, more rearing and sniffing of the experimenter observed in *Shank3* mutant dogs (Fig. 2h, i, Fig. S6, and Table S8 online). Moreover, *Shank3* mutant dogs showed a significantly longer interaction duration with the experimenter either standing (phase 1, 2 min) or crouching (phase 2, 2 min) after PTZ administration compared with saline administration (Fig. 2i and Table S8 online). These results indicate a positive effect of PTZ treatment on social interactions in *Shank3* mutant dogs.

Altogether, we for the first time examined behavioral and electrophysiological phenotypes related to somatosensory processing in a dog model carrying autism-associated *Shank3* mutations. We found that heterozygous *Shank3* mutant dogs exhibited reduced tactile reactivity, cortical responses, and resting state brain oscillations. Importantly, we found that PTZ, a $GABA_A$ receptor antagonist, was capable of reversing these reduced behavioral and electrophysiological phenotypes as well as social interaction impairment in *Shank3* mutant dogs. Furthermore, the spectral powers of resting-state brain oscillations at most frequencies exhibited significant correlations, not only with tactile sensitivity but also with locomotor activity and social interaction duration in *Shank3* mutants and WT dogs (Tables S9 and S10 online). Our findings support that the *Shank3* mutant dog is a valid model to investigate sensory issues associated with ASD as *Shank3* mutant dogs faithfully recapitulate the clinical features of ASD patients and allow us to dissect a mechanistic link between impaired sensory processing and core autistic behaviors. The rescue effects of the $GABA_A$ receptor antagonist PTZ for both sensory processing and autistic behaviors suggest a close connection between tactile responses and social interactions, and a potential therapeutic targeting GABA-associated signaling pathway for *SHANK3*-associated disorders or broadly for sensory issues of idiopathic ASD.

Conflict of interest

The authors declare that they have no conflict of interest.

Acknowledgments

We thank Qingjian Han for the discussion and Tianzi Jiang's laboratory for providing a stimulator. This work was supported by the National Key Research and Development Program (2019YFA0707100 and 2021ZD0203901), the National Natural Science Foundation of China (31830036, 31921002, and 32071061), the Beijing Natural Science Foundation (JQ22018), and the Spring City Plan (2022SCP001).

Author contributions

Qi Shi and Liang Wu designed and performed experiments. Qi Shi and Baolong Ren analyzed data. Qi Shi, Li Hu, and Yong Q. Zhang wrote the manuscript. Kun Guo, Yong-Hui Jiang, Li Hu, and Yong Q. Zhang revised the manuscript. Li Hu and Yong Q. Zhang contributed equally to this work as supervisors.

Appendix A. Supplementary material

Supplementary data to this article can be found online at https://doi.org/10.1016/j.scib.2024.09.011.

References

[1] Tomchek SD, Dunn W. Sensory processing in children with and without autism: A comparative study using the short sensory profile. Am J Occup Ther 2007;61:190–200.

[2] Mikkelsen M, Wodka EL, Mostofsky SH, et al. Autism spectrum disorder in the scope of tactile processing. Dev Cogn Neurosci 2018;29:140–50.

[3] Tavassoli T, Layton C, Levy T, et al. Sensory reactivity phenotype in Phelan-McDermid Syndrome is distinct from idiopathic ASD. Genes (Basel) 2021;12:977.

[4] Chen Q, Deister CA, Gao X, et al. Dysfunction of cortical GABAergic neurons leads to sensory hyper-reactivity in a Shank3 mouse model of ASD. Nat Neurosci 2020;23:520–32.

[5] Orefice LL, Mosko JR, Morency DT, et al. Targeting peripheral somatosensory neurons to improve tactile-related phenotypes in ASD models. Cell 2019;178:867–86.

[6] Drapeau E, Riad M, Kajiwara Y, et al. Behavioral phenotyping of an improved mouse model of Phelan-McDermid syndrome with a complete deletion of the *Shank3* gene. eNeuro 2018;5:ENEURO.0046-18.

[7] Foss-Feig JH, Heacock JL, Cascio CJ. Tactile responsiveness patterns and their association with core features in autism spectrum disorders. Res Autism Spectr Disord 2012;6:337–44.

[8] Tasnim A, Alkislar I, Hakim R, et al. The developmental timing of spinal touch processing alterations predicts behavioral changes in genetic mouse models of autism spectrum disorders. Nat Neurosci 2024;27:484–96.

[9] Cao X, Liu WP, Cheng LG, et al. Whole genome analyses reveal significant convergence in obsessive-compulsive disorder between humans and dogs. Sci Bull 2021;66:187–96.

[10] Tian R, Li Y, Zhao H, et al. Modeling SHANK3-associated autism spectrum disorder in Beagle dogs via CRISPR/Cas9 gene editing. Mol Psychiatry 2023;28:3739–50.

[11] Czeibert K, Andics A, Petneházy Ö, et al. A detailed canine brain label map for neuroimaging analysis. Biol Futur 2019;70:112–20.

[12] Macerollo A, Brown MJN, Kilner JM, et al. Neurophysiological changes measured using somatosensory evoked potentials. Trends Neurosci 2018;41:294–310.

[13] Angel RW, Quick WM, Curtis Boylls C, et al. Decrement of somatosensory evoked potentials during repetitive stimulation. Electroencephalogr Clin Neurophysiol 1985;60:335–42.

[14] Mazaheri A, Nieuwenhuis ILC, van Dijk H, et al. Prestimulus alpha and mu activity predicts failure to inhibit motor responses. Hum Brain Mapp 2009;30:1791–800.

[15] Yamazaki M, Honda S, Tamaki K, et al. Effects of (+)-bicuculline, a GABAa receptor antagonist, on auditory steady state response in free-moving rats. PLoS One 2020;15:e0236363.

[16] Bircher RP, Kanai T, Wang SC. Intravenous, cortical and intraventricular dose-effect relationship of pentylenetetrazol, picrotoxin and deslanoside in dogs. Electroencephalogr Clin Neurophysiol 1962;14:256–67.